

Chapter 5

Dielectric permittivity estimation for liquids

The previous chapter has proposed a free space method to estimate complex relative dielectric permittivity of homogeneous, isotropic non-magnetic solid materials. The method has proved accuracy on several material samples. However, solid materials is only one among the types of materials used in human life. Liquid also is one of the common states of existence of substances that we encounter every day. In several fields of research and industries, such as water quality research, brewery, chemical industry and etc., a good understanding on the dispersion properties of water-based liquids would deliver more insights and hints for further improvements and discoveries. This chapter will introduce the analysis and the process of permittivity estimation dealing with water-based liquids based on the free space method, with water as an example.

5.1 Introduction

Complex dielectric permittivity estimation of liquids is one of the major problems in dielectric characterization. Several well-known methods have been proposed, such as the resonator methods, the waveguide methods or the open-ended coaxial probe method. With the growing demand of a non-destructive, non-contacting and broadband permittivity measurement techniques, to conduct measurements at high temperatures, or to deal with chemically active liquids or to support the development of biomedical techniques, remote sensing and etc., the traditional methods face several limits.

In this context, the free space techniques appear to be an attractive way to cope with the demand. One of the notable effort using the free space techniques to deal with liquids is the work of Ghodgaonkar et al [16]. In [16], an analytical approach was introduced to calculate the relative permittivity of solid materials. To secure the uniqueness of the solution, the sample thickness was required to be very thin, a condition which, in turns, requires a sandwich structure to prevent the material sample from sagging. Such a structure, however, can be used to measure liquids as well. The idea was later investigated by the author's group.

The analytic method of Ghodgaonkar et al is general in the sense that it can be applied to solids, powders and liquids and it can calculate both permittivity and permeability. However, it requires two scattering parameters with several complex calculations and need to use thin material samples to secure the uniqueness of the solutions. In the cases of non-magnetic and high loss liquids, in particular water-based liquids, it is possible to use a more simple analytical free space method using only the reflection coefficient and other known information.

In this research, we propose an analytical free space methods to calculate the relative dielectric permittivity ϵ_r of high loss liquids from the multiple reflection coefficient Γ_m of the sample obtained from measurement. ϵ_r of water was estimated as an example. Promising results were obtained.

5.2 Scattering analysis

5.2.1 Some differences compared to the case of a solid material

Considering two cases of solid materials and liquids, the later case requires more complex analysis. In the previous chapter, the process of relative permittivity estimation on a solid cube was explained. Because of the solid nature, the material under test can be machined into a sharp cubic form and it can stand alone during measurement. Therefore, from the measurement one can obtain a relatively pure scattering field from the material of interest. From that data, one can immediately analyze to get the wanted relative permittivity. Meanwhile, the case is a little more complicated for a liquid because a liquid sample needs to be stored in a container before one makes a measurement. In this research, aiming to use the free space method, a liquid even needs to be shaped into cubic form to facilitate our analysis. Since the container has dimensions and the container's material has permittivity and permeability, the container will contribute inevitably to the scattering field one may obtain. Therefore, the scattering analysis needs to separate the scattering contribution from the container in order to have a direct relation between the scattering quantity and the liquid's relative permittivity.

There is one more point that requires attention is the lossy nature of water and water-based liquids. Numerous research have revealed that the relative permittivity of water has a large imaginary part which results in quick attenuation of electromagnetic fields in water and water-based liquids. That means if the container is large enough, electromagnetic fields will be attenuated entirely inside the container and the multiple reflection that causes difficulties in the case of low-loss solid materials will not occur.

The above two points will be considered and used in the following sections.

5.2.2 The decomposition of the scattering container

Figure 5.1a shows the model of a container used in this research. It has a rectangular cylinder shape with a rectangular cylinder empty space to contain the liquid for measurement. A liquid would fill in the container and would form a rectangular cylinder object with an empty top space. When an electromagnetic wave illuminates the container in the normal specular direction of the S1 surface, it is assumed that the container can be separated into 5 parts, namely top, sides, bottom and center as shown in Fig. 5.1(b) and the scattering field from the container in that specific direction can be calculated approximately by taking the sum of scattering contributions from the 5 parts. In Fig. 5.1(b), one may realize that all the parts are of the shapes that a scattering far field formulation can be formulated with high accuracy in the normal specular direction of S1 surface. In the following discussions, the bottom, the two sides and the top part will be referred together as the frame of the container.

As can be seen in Fig. 5.1(b), the scattering contribution from the frame would provide us information only about the container's material. Meanwhile, from the center part we may be able to establish a relation between the liquid's relative permittivity and other factor that enables an analysis to calculate the wanted relative permittivity from measurement data. Therefore, if the assumptions hold we will be able to separate the unwanted scattering contributions from the frame to obtain only the scattering field from the center part of the container and to conduct further analyses. In the next discussions, the scattering analysis and feasibility of our assumptions will be discussed.

5.2.3 Scattering analysis and validation

We consider the case when a TE polarized electromagnetic plane wave illuminates the container in the normal specular direction. Using the theory presented in Chapter 3, the complex far field scattering quantities of the bottom and the two sides in the same direction can be determined by the following equations. In the following

calculation the reference plane is the S1 surface.

$$\hat{\sigma}_b = -\frac{ik}{\sqrt{\pi}}w_1t\Gamma_m \quad (5.1)$$

$$\hat{\sigma}_s = -\frac{2ik}{\sqrt{\pi}}l_2t\Gamma_m \quad (5.2)$$

$$\Gamma_m = \frac{\Gamma_s(1 - e^{i2kd\sqrt{\varepsilon_r}})}{1 - \Gamma_s^2 e^{i2kd\sqrt{\varepsilon_r}}}$$

$$\Gamma_s = \frac{\sqrt{\varepsilon_r} - 1}{\sqrt{\varepsilon_r} + 1}$$

Here $\hat{\sigma}_b$ and $\hat{\sigma}_s$ are the complex scattering quantities from the bottom and the two sides of the container, respectively. Γ_m and Γ_s are the multiple and the single surface reflection coefficients. ε_r is the complex relative permittivity of the container's material. k is the wave number in free space.

Before considering the center and top parts of the container, we shall consider the normal reflection from a structure which consists of 5 infinite dielectric layers illuminated by a TE polarized electromagnetic plane wave as shown in Fig. 5.2(a). By using the impedance propagation method, the reflection coefficient in the normal specular direction at the surface of reflection can be calculated by the following equations.

$$\Gamma_m[z = 0^+] = \frac{Z_{in}[z = 0^-] - \eta_1}{Z_{in}[z = 0^-] + \eta_1} \quad (5.3)$$

$$Z_{in}[z = 0^-] = \eta_2 \frac{1 + \Gamma_{in}[z = 0^-]}{1 - \Gamma_{in}[z = 0^-]}$$

$$\Gamma[z = 0^-] = \Gamma[z = -a^+]e^{i2ka\sqrt{\varepsilon_{r2}}}$$

$$\Gamma[z = -a^+] = \frac{Z_{in}[z = -a^-] - \eta_2}{Z_{in}[z = -a^-] + \eta_2}$$

$$Z_{in}[z = -a^-] = \eta_3 \frac{1 + \Gamma[z = -a^-]}{1 - \Gamma[z = -a^-]}$$

$$\Gamma[z = -a^-] = \Gamma[z = -(a+b)^+]e^{i2kb\sqrt{\varepsilon_{r3}}} \quad (5.4)$$

$$\Gamma[z = -(a+b)^+] = \frac{Z_{in}[z = -(a+b)^-] - \eta_3}{Z_{in}[z = -(a+b)^-] + \eta_3} \quad (5.5)$$

$$\begin{aligned}
Z_{in}[z = -(a+b)^-] &= \eta_4 \frac{1 + \Gamma[z = -(a+b)^-]}{1 - \Gamma[z = -(a+b)^-]} \\
\Gamma[z = -(a+b)^-] &= \Gamma[z = -(a+b+c)^+] e^{i2kc\sqrt{\varepsilon_{r4}}} \\
\Gamma[z = -(a+b+c)^+] &= \frac{\eta_5 - \eta_4}{\eta_5 + \eta_4} \\
\eta_i &= \sqrt{\frac{\mu_{ri}}{\varepsilon_{ri}}}
\end{aligned}$$

One may realize that the center and the top parts of the container also can be represented by two 5-layer dielectric structures as seen in Fig. 5.2(b). Although they are finite structures, the multiple reflection coefficients Γ_{mt} and Γ_{mc} from the top and center parts in the normal specular reflection direction of S1 surface can be represented in the manner of Eq. (5.3). Then, the complex far field scattering quantities of the center and top parts can be given by the following equations.

$$\hat{\sigma}_c = -\frac{ik}{\sqrt{\pi}}wl\Gamma_{mc} \quad (5.6)$$

$$\hat{\sigma}_t = -\frac{ik}{\sqrt{\pi}}wl_1\Gamma_{mt} \quad (5.7)$$

In order to validate the assumptions made before, the theoretical complex far field scattering quantities of a real container will be calculated when it is filled with water. Then the results are compared to the measurement results. The dimensions of the container parts are shown in Table 5.1. Here, the complex relative permittivity of acrylic is the average value (2.578, 0.035) estimated in the frequency range 18–26 GHz. Water's relative permittivity at 22°C is obtained using the model of Stogryn [37], as shown in Fig. 5.3. This theoretical relative permittivity reference has been confirmed by several experiment results as shown in Fig. 5.4.

The theoretical complex far field scattering quantities of the containers' parts and the total contribution from the whole container are calculated and shown in Fig. 5.5. A comparison between the theoretical complex far field scattering quantity of the container and measurement is shown in Fig. 5.6. After compensating the phase of measurement data, it can be seen that the theoretical real and imaginary parts resemble closely the measured values. Therefore, it can be concluded that when

the container is illuminated by a TE polarized plane wave in the normal specular direction of S1 surface, the complex far field scattering quantity of the container can be obtain approximately by taking the sum of the complex far field scattering quantities from the proposed parts. A comparison between the measured complex scattering quantity and the theoretical one of an empty container (or container filled with air) is shown in Fig. 5.7. The theoretical values were calculated with acrylic's relative permittivity taken as (2.578,0.035) in the whole frequency range.

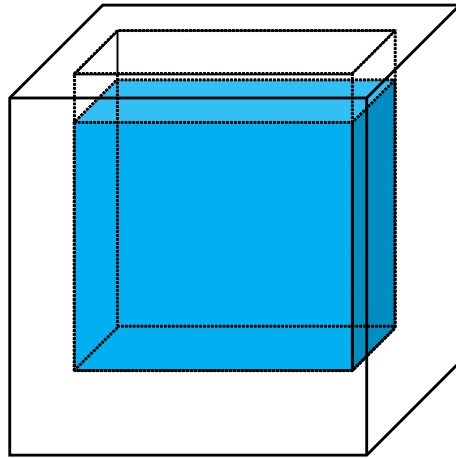
Table 5.1: Dimensions of the components of the container

Name	Length [mm]	Width [mm]	Thickness [mm]
Bottom part	$w_1 = 102.0$	$t = 1.0$	$d = 32.0$
Side part	$l_2 = 105.0$	$t = 1.0$	$d = 32.0$
Top part	$w = 100.0$	$l_1 = 5.0$	$a = 1.0, b = 30.0, c = 1.0$
Center part	$l = 100.0$	$w = 100.0$	$a = 1.0, b = 30.0, c = 1.0$

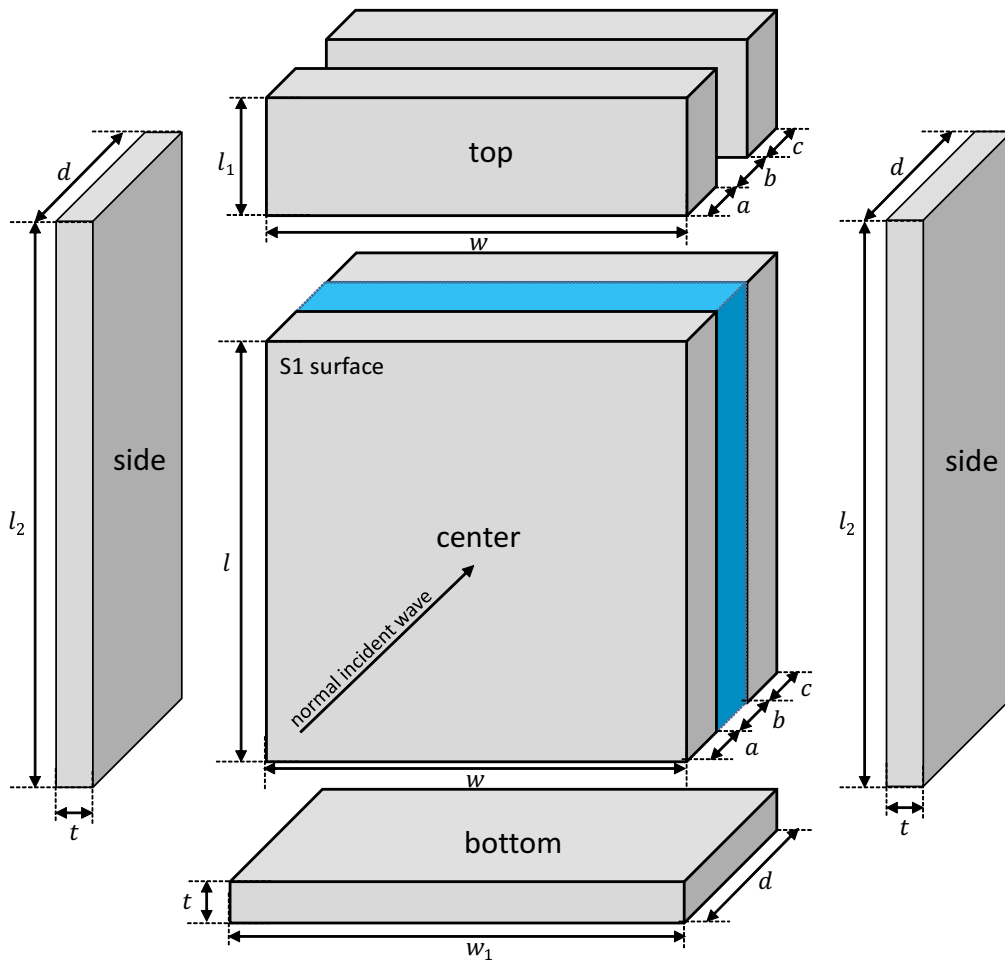
As mentioned in Subsection 5.2.1, water and water-based liquids have a large permittivity loss leading to large attenuation of electromagnetic energy inside the liquid-filled container. With that understanding, it can be predicted that when the thickness of the liquid layer of the container is large enough, multiple reflection effect can be reduced to the extend as if the liquid layer is infinitely thick. In that case, the structure of the center part of the container can be represented by a 3-layer model shown in Fig. 5.8. That also allows the multiple reflection coefficient at S1 surface to be calculated by the following equation.

$$\Gamma_m = \frac{\frac{1-\sqrt{\epsilon_{r1}}}{1+\sqrt{\epsilon_{r1}}} + \frac{\sqrt{\epsilon_{r1}}-\sqrt{\epsilon_{r2}}}{\sqrt{\epsilon_{r1}}+\sqrt{\epsilon_{r2}}} e^{2ika\sqrt{\epsilon_{r1}}}}{1 + \frac{1-\sqrt{\epsilon_{r1}}}{1+\sqrt{\epsilon_{r1}}} \frac{\sqrt{\epsilon_{r1}}-\sqrt{\epsilon_{r2}}}{\sqrt{\epsilon_{r1}}+\sqrt{\epsilon_{r2}}} e^{2ika\sqrt{\epsilon_{r1}}}} \quad (5.8)$$

We have compared the numerical values of the reflection coefficients of the water-filled center part using the 5-layer and the 3-layer models by varying the thickness b from 1 mm to several centimeters, as can be seen in Figs. 5.9, 5.10. It has been observed that when b is larger than a few millimeters in this frequency band from 18 to 26 GHz, the reflection coefficient by the 5-layer model quickly converges to the coefficient by the 3-layer model. Based on this observation, we set the thickness of the liquid layer in the container to 30.0 mm so that the reflection coefficient from the center part can be calculated by the 3-layer model. In a little more general view, if $2kb\text{Im}[\sqrt{\varepsilon_{r3}}]$ gets large then $e^{i2kb\sqrt{\varepsilon_{r3}}}$ and the right hand side of Eq. (5.4) rapidly approaches 0. Accordingly, the effects from the later layers of the 5-layer model represented by Eq. (5.5) disappears. Depending on the accuracy demanded, $2kb\text{Im}[\sqrt{\varepsilon_{r3}}]$ can be increased. To secure the $e^{i2kb\sqrt{\varepsilon_{r3}}}$ to be less than 10^{-6} , one may want to have $2kb\text{Im}[\sqrt{\varepsilon_{r3}}] > 15$.

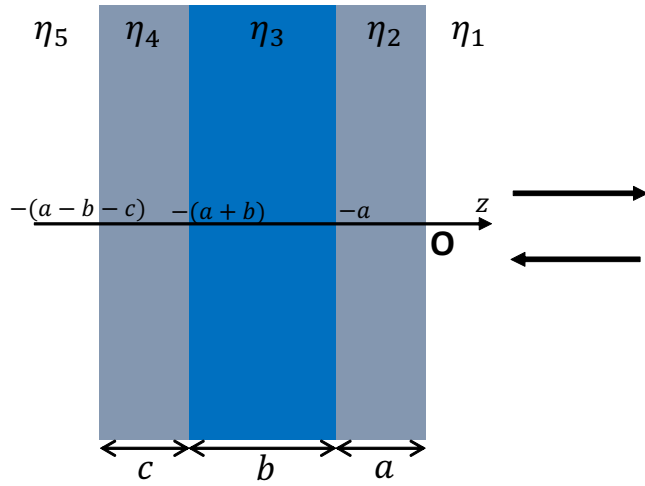


(a) Model of a container with a liquid inside

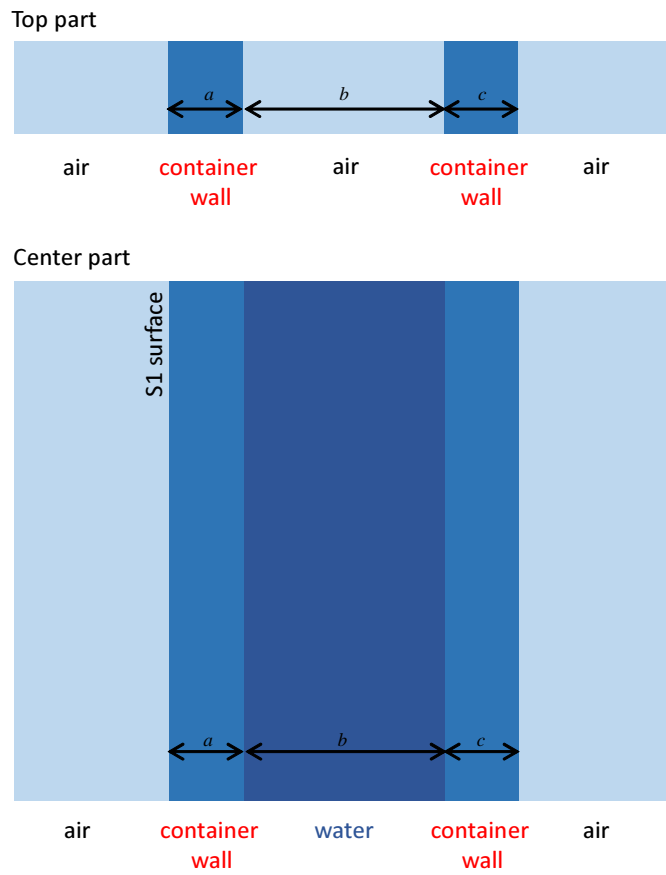


(b) The decomposition of a container

Figure 5.1: Scattering model for the liquid container.

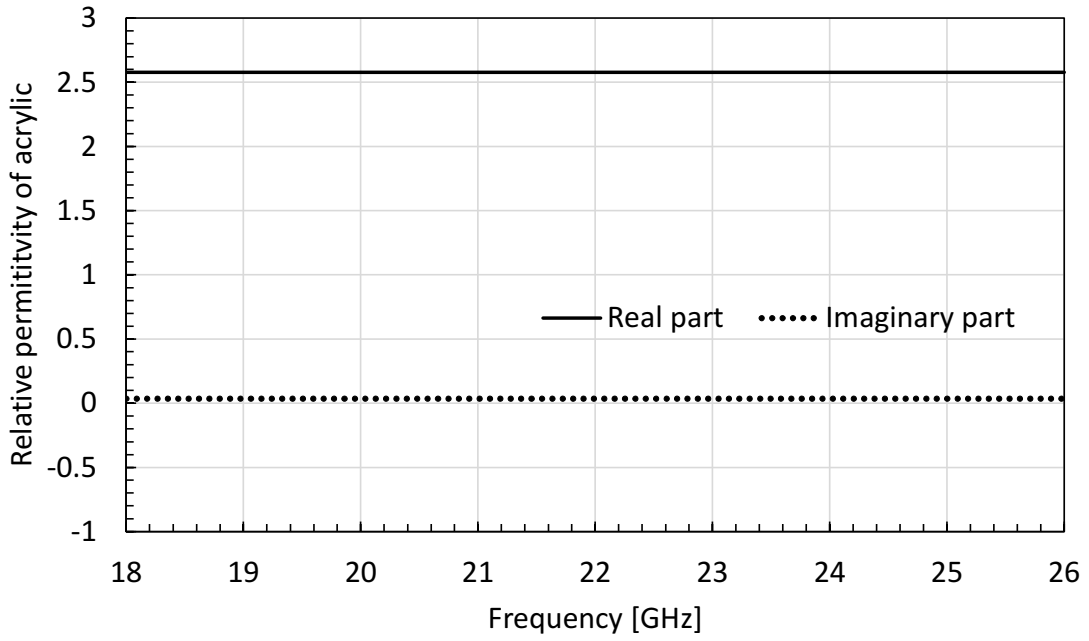


(a) Model of a 5-layers dielectric structure

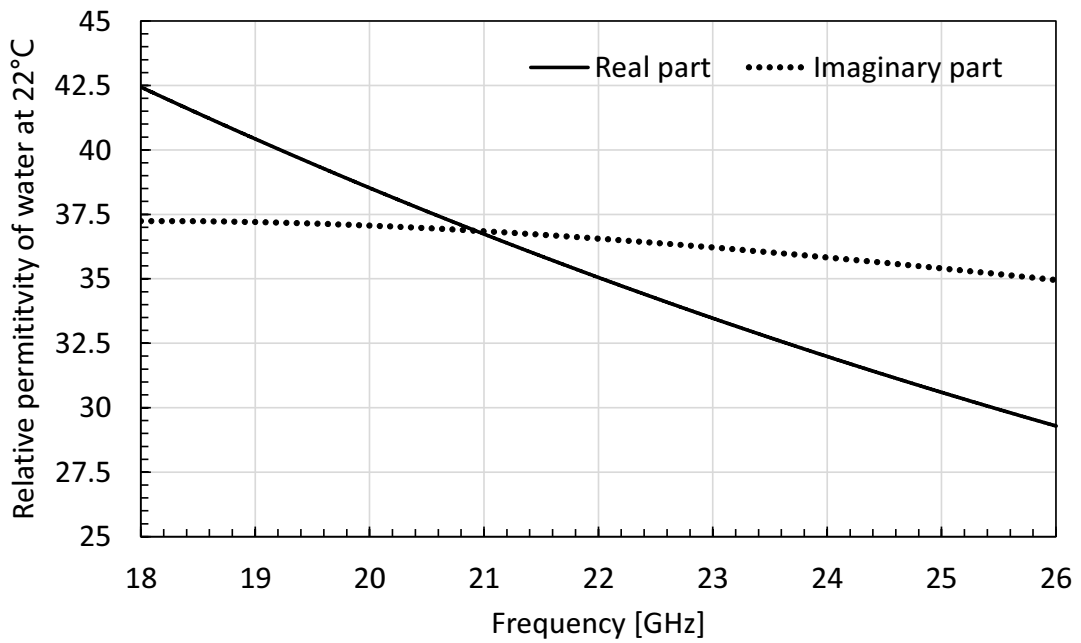


(b) Structures of the top and center parts

Figure 5.2: Multiple-layer dielectric structures for scattering analysis.

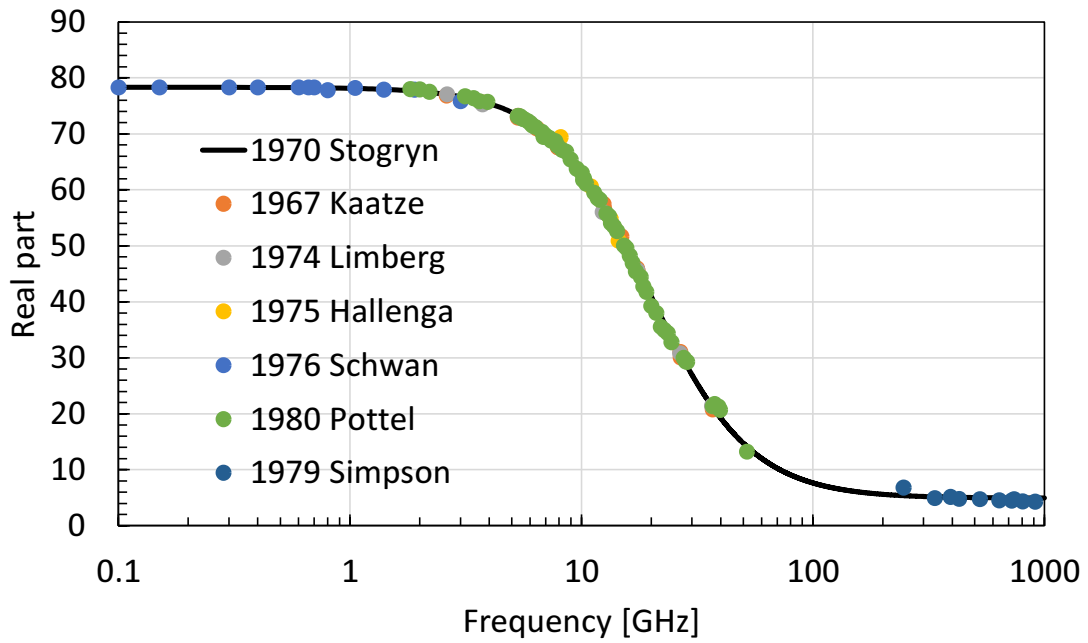


(a) Complex relative permittivity of the acrylic container

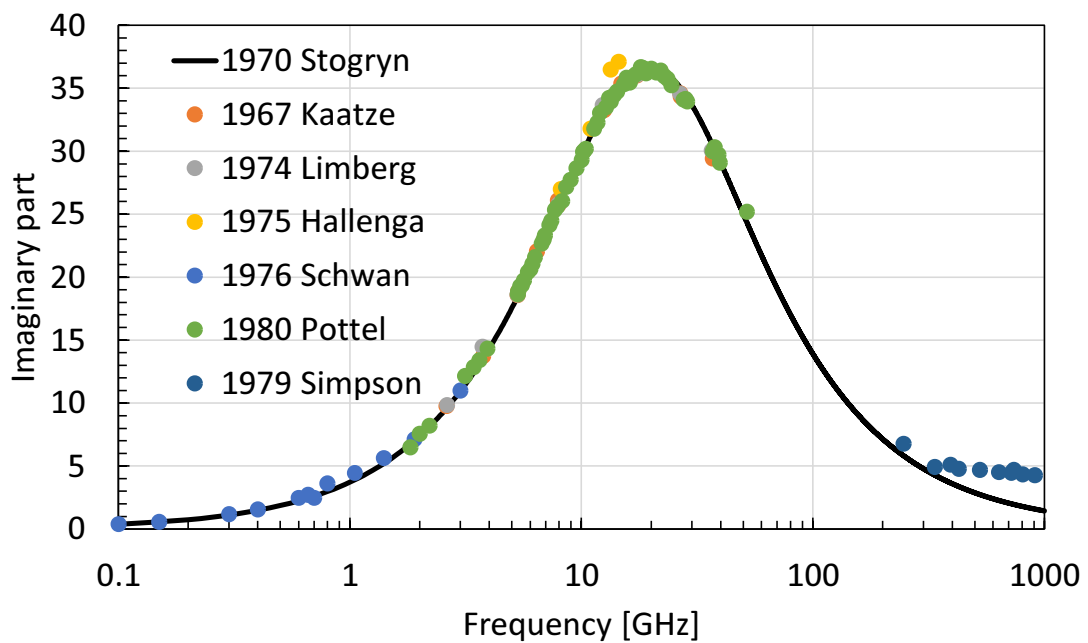


(b) Complex relative permittivity of water- Debye model [37]

Figure 5.3: Complex relative permittivities of container's material and water at 22°C.

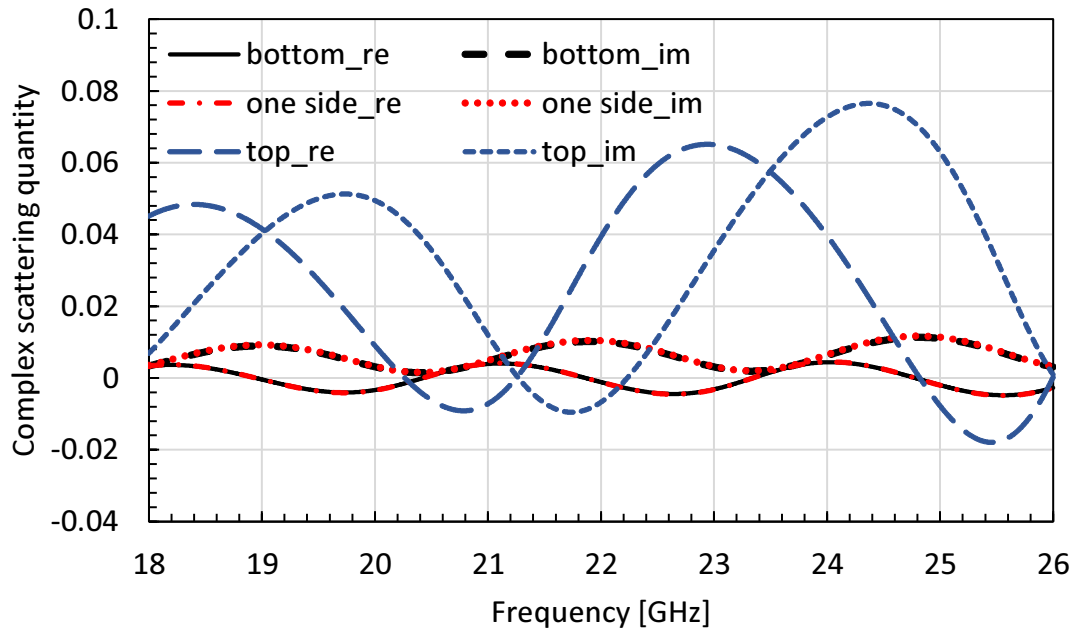


(a) The real part of water ϵ_r

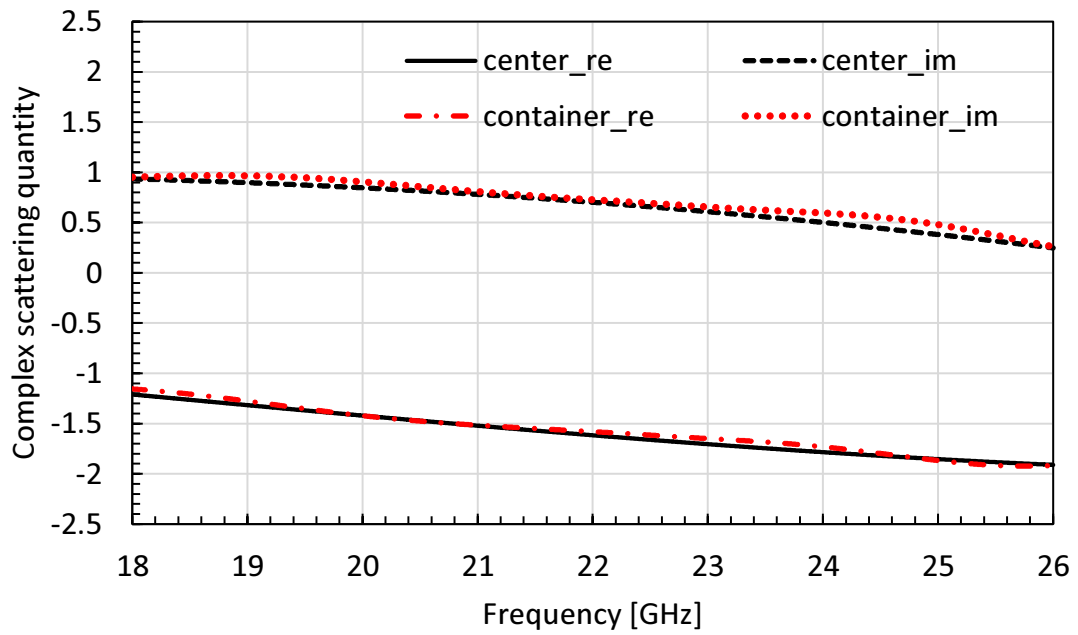


(b) The imaginary part of water ϵ_r

Figure 5.4: Debye model of the relative permittivity of water at 22°C by Stogryn in a comparison with contemporary results [37].

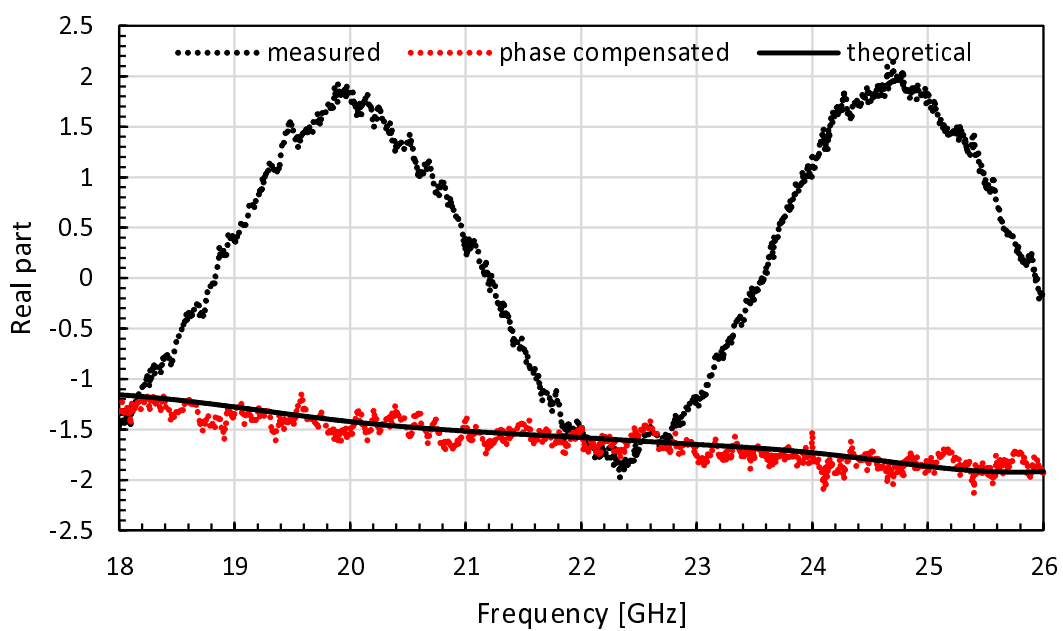


(a) Complex far field scattering quantities of the bottom, top and side parts

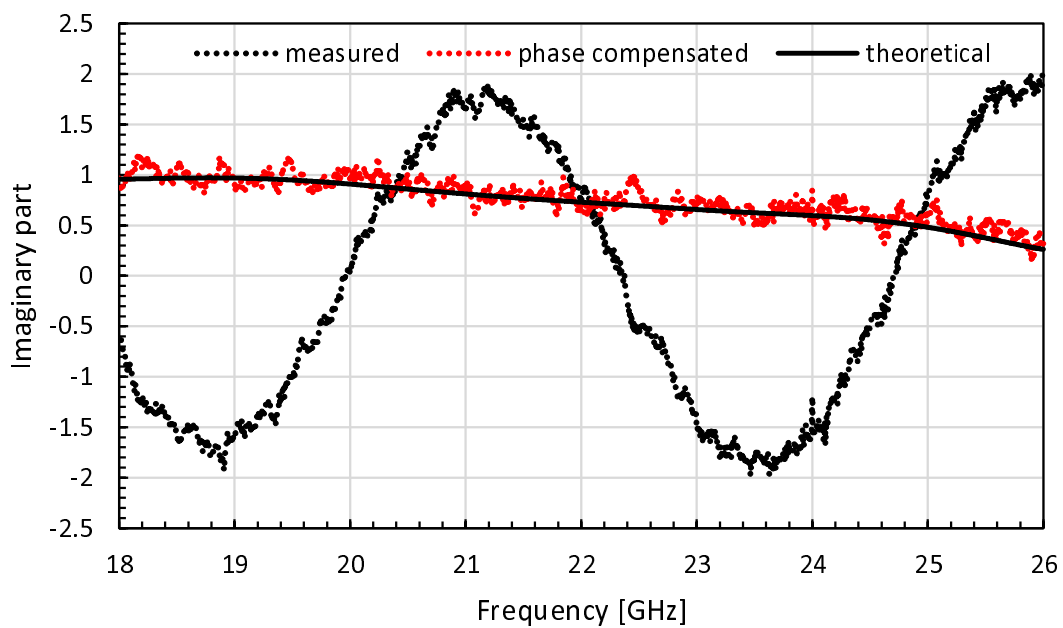


(b) Complex far field scattering quantities of the center part and total contributions

Figure 5.5: Complex far field scattering quantities of each container's part and total contribution.

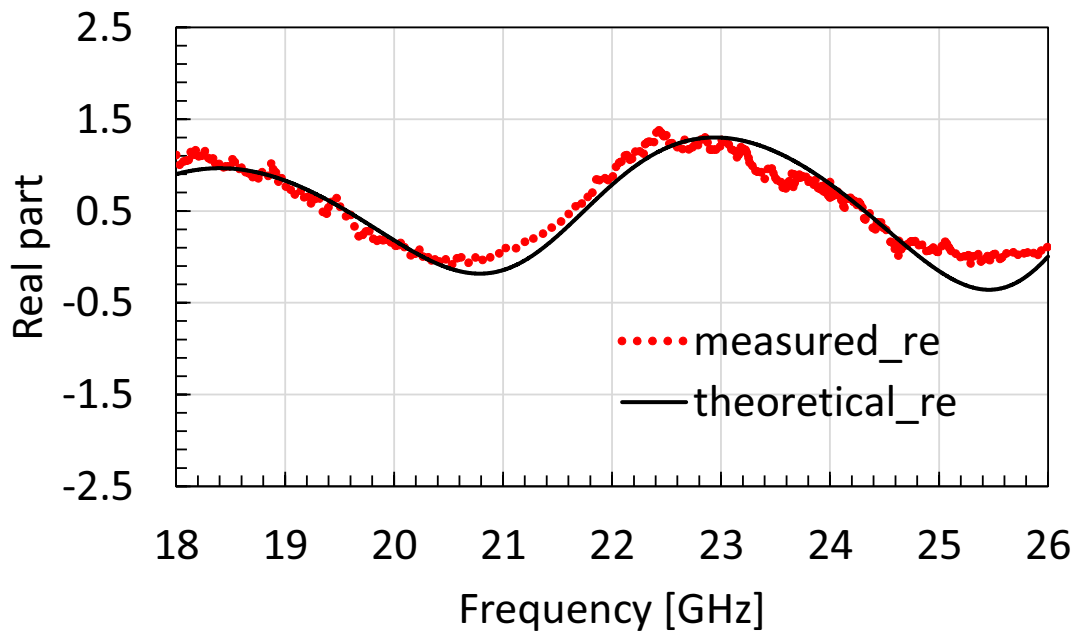


(a) Real parts of complex far field scattering quantities

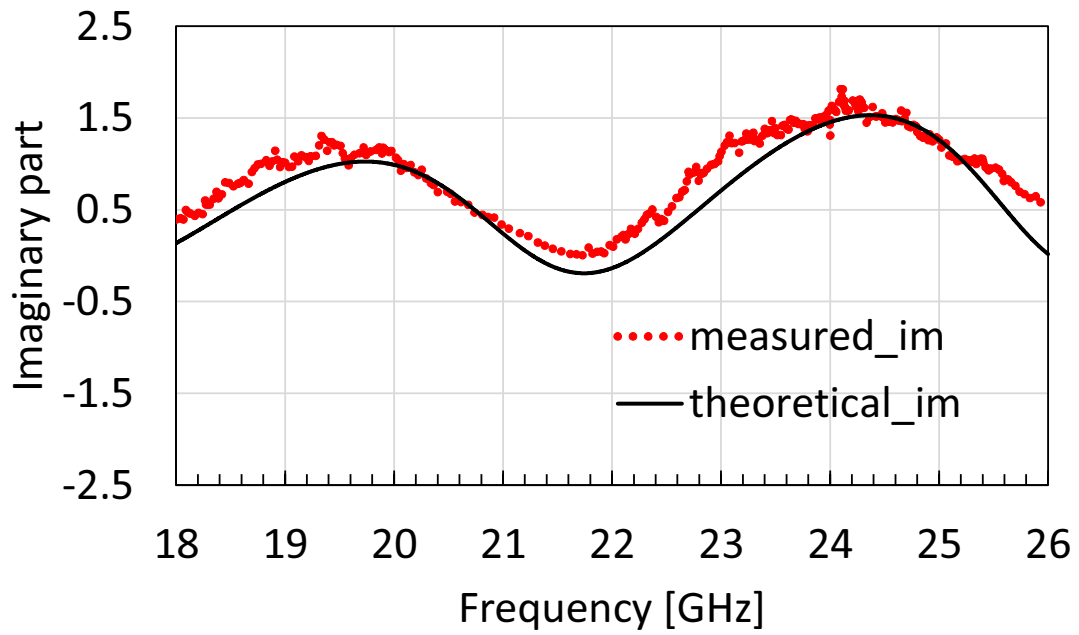


(b) Imaginary parts of complex far field scattering quantities

Figure 5.6: A comparison with measurement.



(a) Real parts of complex far field scattering quantities



(b) Imaginary parts of complex far field scattering quantities

Figure 5.7: The complex scattering quantity of a container filled with air.

3-layer model center part

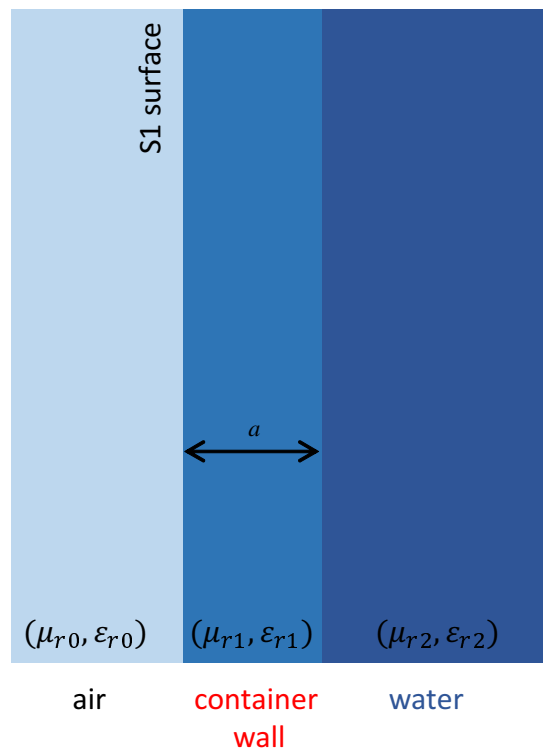


Figure 5.8: Reduced model of the center part of the container.

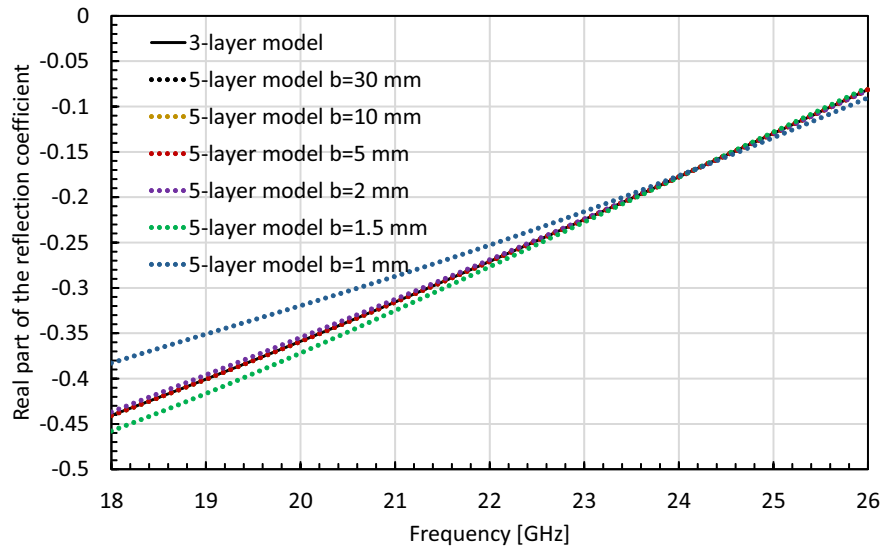


Figure 5.9: Effects of the thickness b on the real part of the reflection coefficient of the center part ($l = w = 100.0$ mm, $a = 1.0$ mm) of a container.

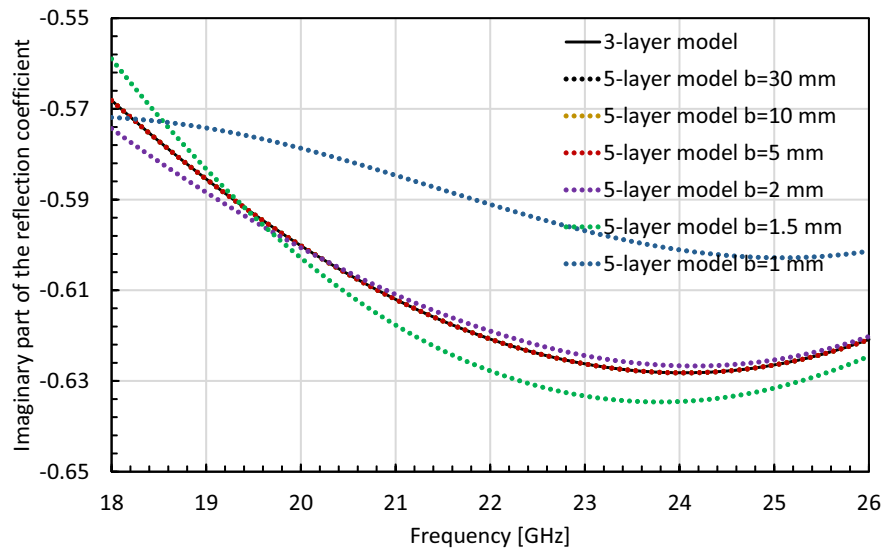


Figure 5.10: Effects of the thickness b on the imaginary part of the reflection coefficient of the center part ($l = w = 100.0$ mm, $a = 1.0$ mm) of a container.

5.3 Permittivity estimation

From Eq. (5.8), one can make a few simple transformations to get

$$\varepsilon_{r2} = \varepsilon_{r1} \left(\frac{1 - A}{1 + A} \right)^2 \quad (5.9)$$

$$A = \frac{\frac{1 - \sqrt{\varepsilon_{r1}}}{1 + \sqrt{\varepsilon_{r1}}} - \Gamma_m}{\Gamma_m \frac{1 - \sqrt{\varepsilon_{r1}}}{1 + \sqrt{\varepsilon_{r1}}} - 1} e^{2ika\sqrt{\varepsilon_{r1}}}. \quad (5.10)$$

One may realize that with a container of known dimensions and material, if the complex far field scattering quantity is obtained from measurement, A is determined. The Eq. (5.9) gives us a direction relation between the liquid permittivity and known information. Based on that, a procedure is devised to obtain the wanted relative permittivity from the measured complex far field scattering quantity.

- 1) Measure the complex far field scattering quantity in the normal specular reflection direction.
- 2) Extract complex scattering far field contribution from the center part of the container. This is obtained by subtracting the theoretical contributions of other parts from the measured scattering quantity.
- 3) Extract the multiple reflection coefficient of the center part and determine the quantity A via Eqs. (5.6),(5.10).
- 4) Calculate the liquid's relative permittivity from known information via Eq. (5.9).

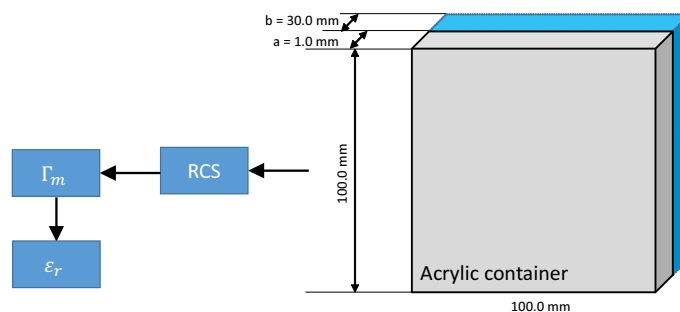


Figure 5.11: Permittivity estimation process.

5.4 Measurements and discussions

5.4.1 Water's relative permittivity

In order to verify the potentials of the proposed procedure, measurements have been conducted with one container with the dimensions described in Table 5.1. A photo of the container on the rotary table can be seen in Fig. 5.12. Estimations have been made when the container was partially filled with water (Case I) and when it is filled fully (Case II). The relative permittivity of acrylic is assumed to be constant in the whole frequency band from 18 to 26 GHz as shown in Fig. 5.3(a).

Figure 5.13 shows that the complex far field scattering quantities of the center part of the container in case I extracted from measurement and theoretical values have good agreement. Estimated water's relative permittivity is shown in Fig. 5.14. Since the measured data oscillated strongly due to noise, averaged values are used to make comparisons. In term of the real part, the sliding average of estimated relative permittivity is close to that by the Debye model. In case II, the same container is filled fully with water and relative permittivity estimation was conducted. In Fig. 5.15, a comparison also suggests a good agreement between the averaged estimated relative permittivity and the relative permittivity obtained from the Debye model. Although significant differences were observed, the two examples have shown the possibility to use my method to estimate the permittivities of water and water-based liquids.

5.4.2 Container's relative permittivity

In the previous subsection, the relative permittivity of acrylic has been assumed to be one value throughout the frequency range. Based on that, the estimated water permittivity's sliding average values has good agreement with the Debye model. To verify those results, one may want to assume that water has the relative permittivity as in the Debye model and to estimate the acrylic's relative permittivity from the measured complex scattering quantity. The result of such an effort is shown in

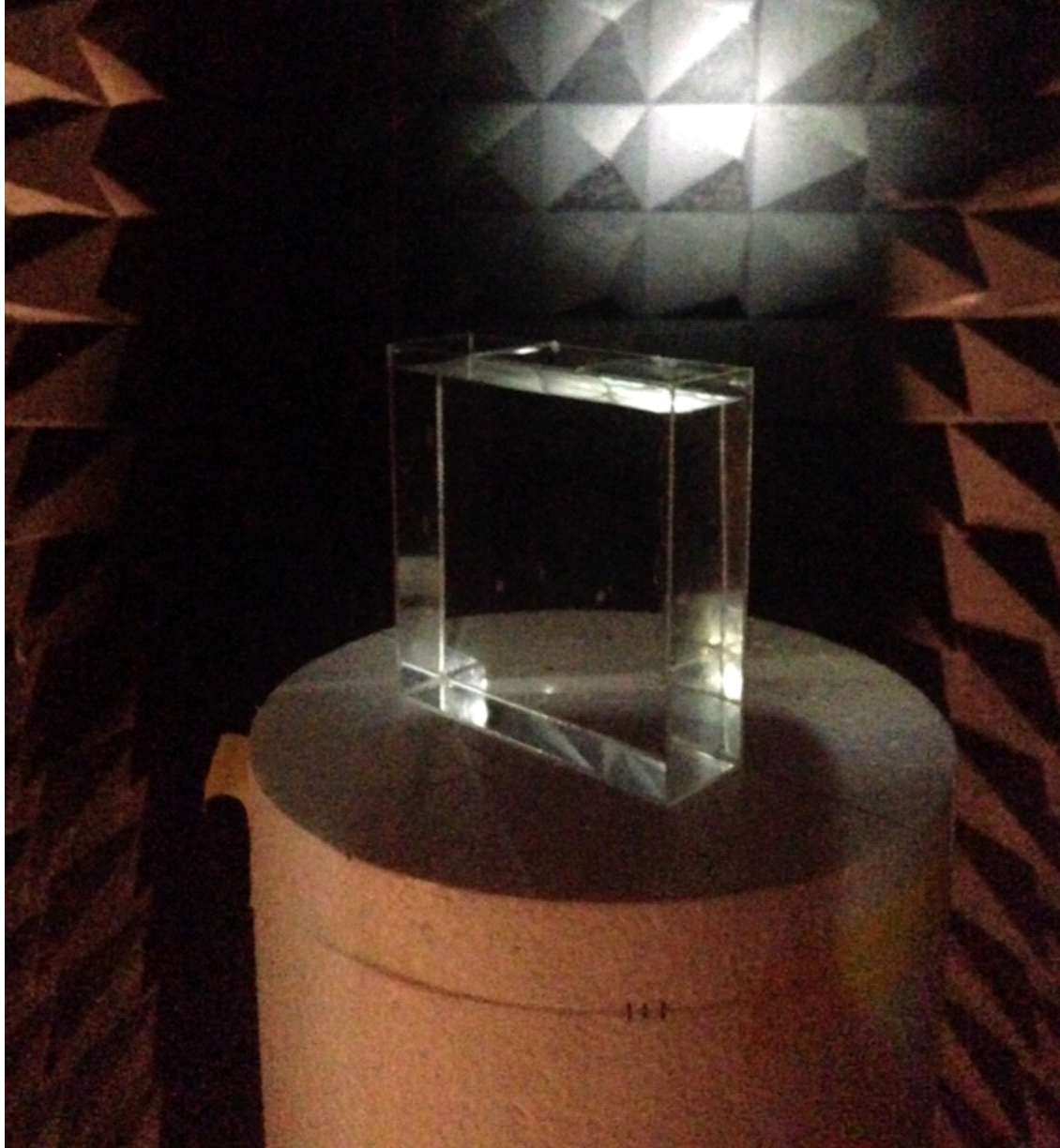
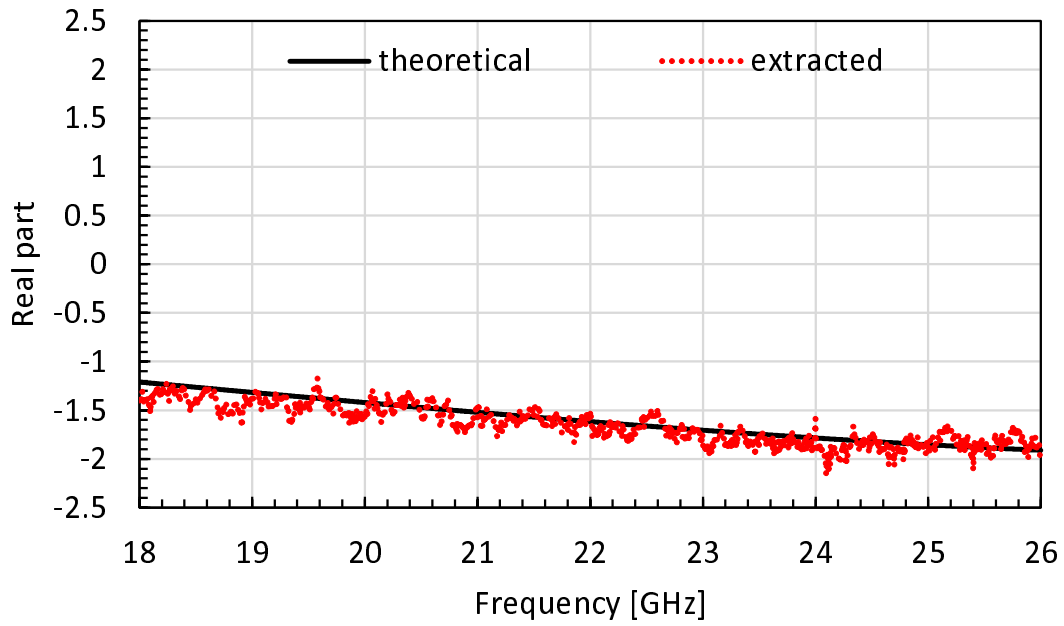
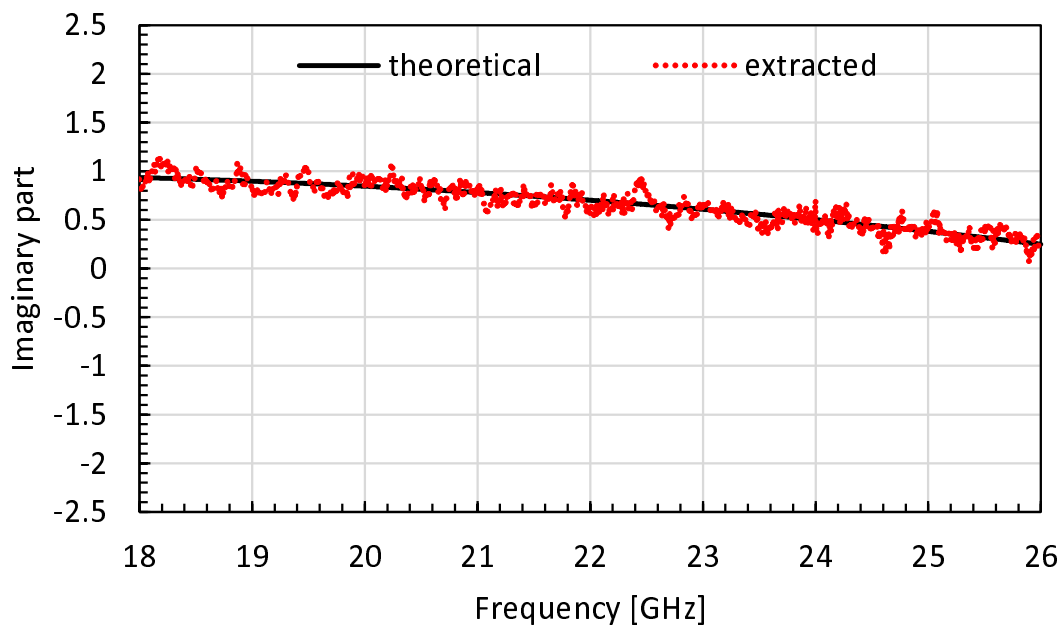


Figure 5.12: The real container used for measurement.

Fig. 5.16. It can be seen that the estimated acrylic permittivity's sliding average value is very close to the reference value (2.578, 0.035).

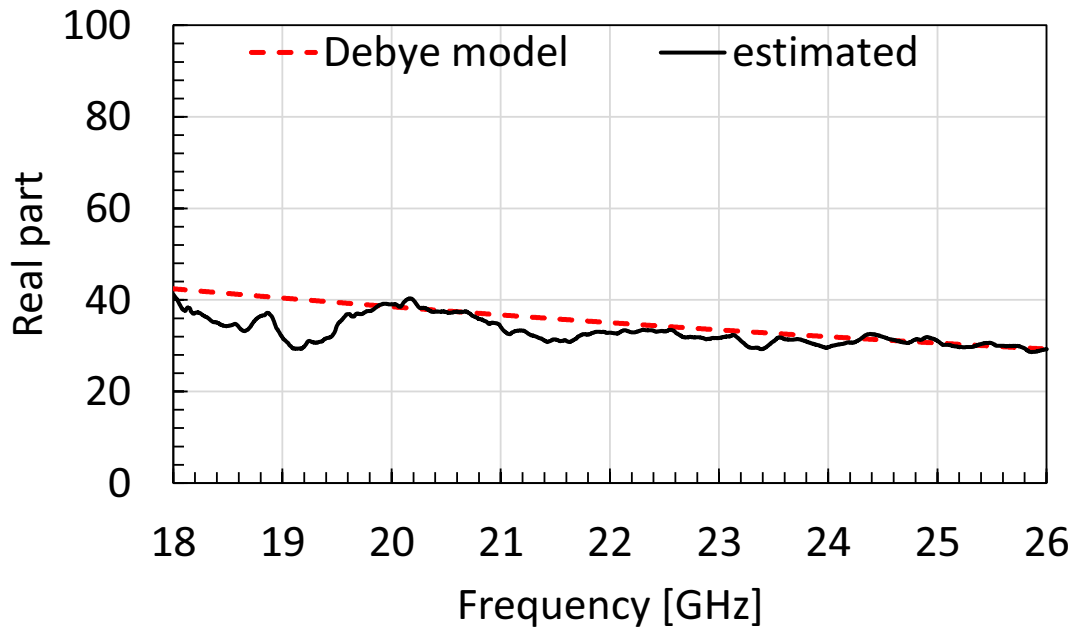


(a) Real parts of complex far field scattering quantities

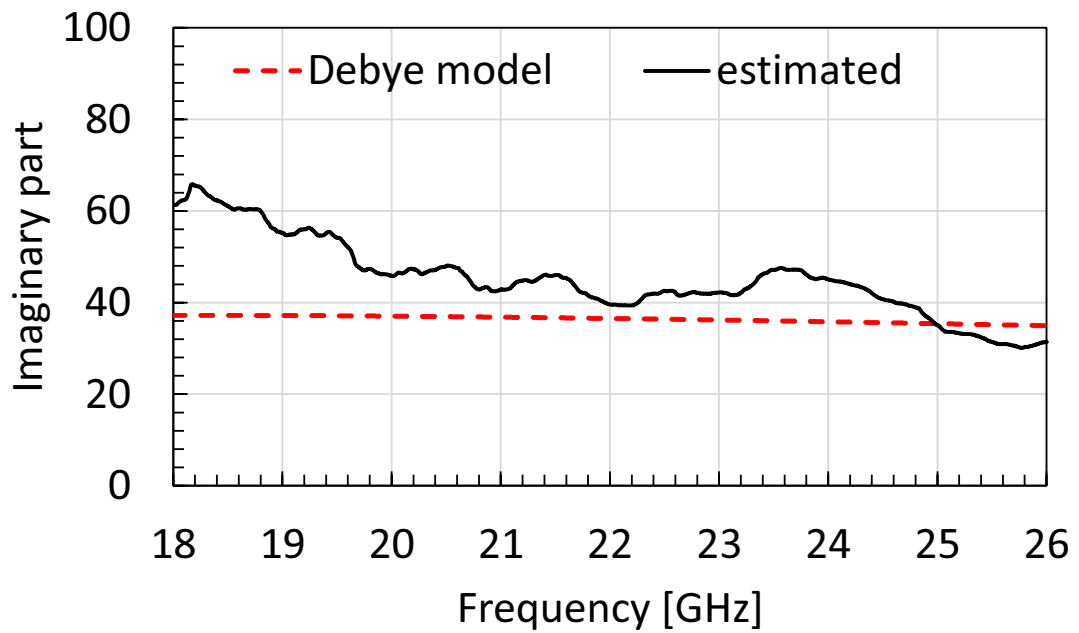


(b) Imaginary parts of complex far field scattering quantities

Figure 5.13: Theoretical and extracted complex far field scattering quantities of the center part- Case I.

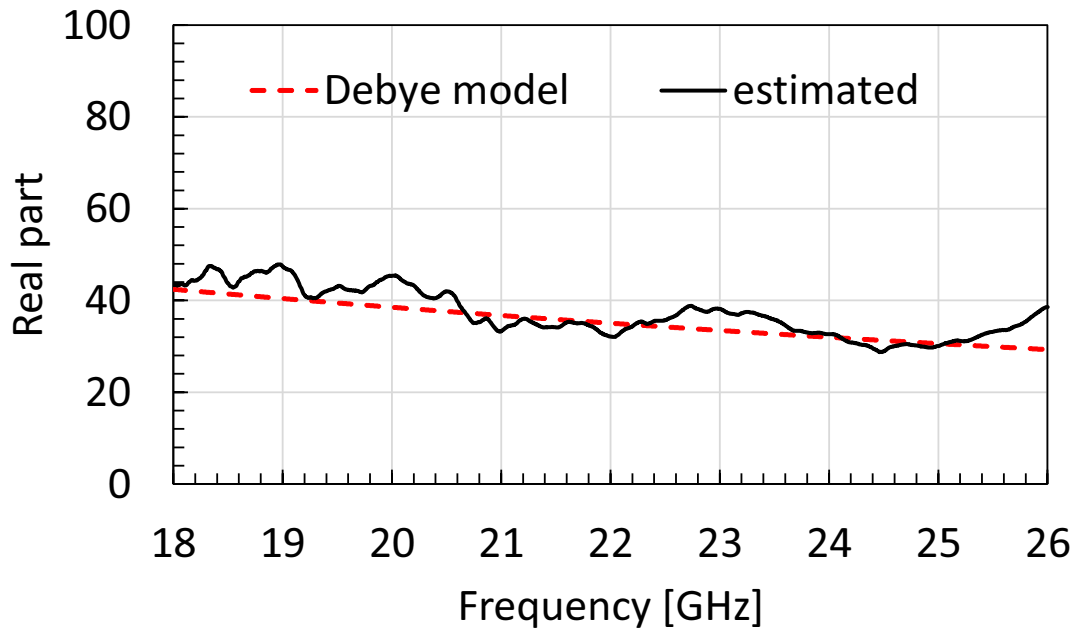


(a) Real parts of water ϵ_r

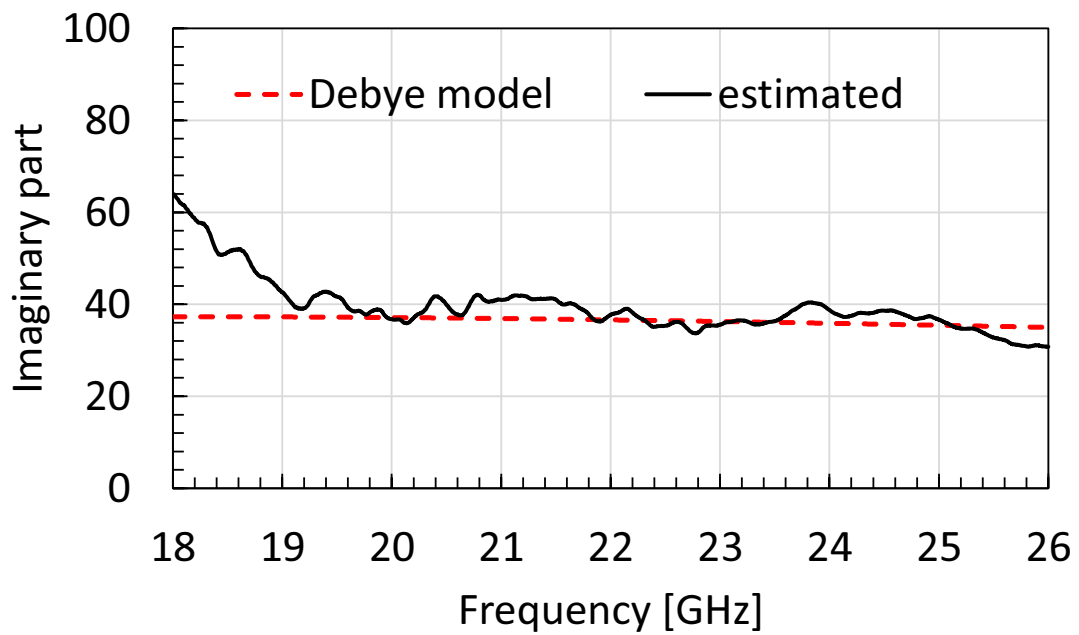


(b) Imaginary parts of water ϵ_r

Figure 5.14: Complex relative permittivity of water estimated from the partially filled container- Case I.

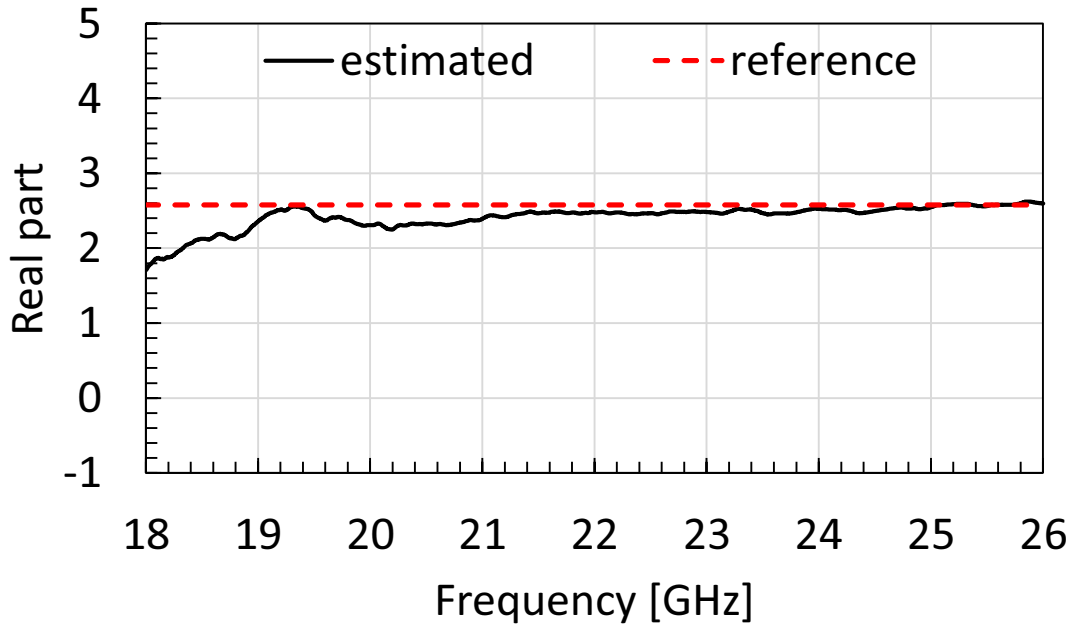


(a) Real parts of water ϵ_r

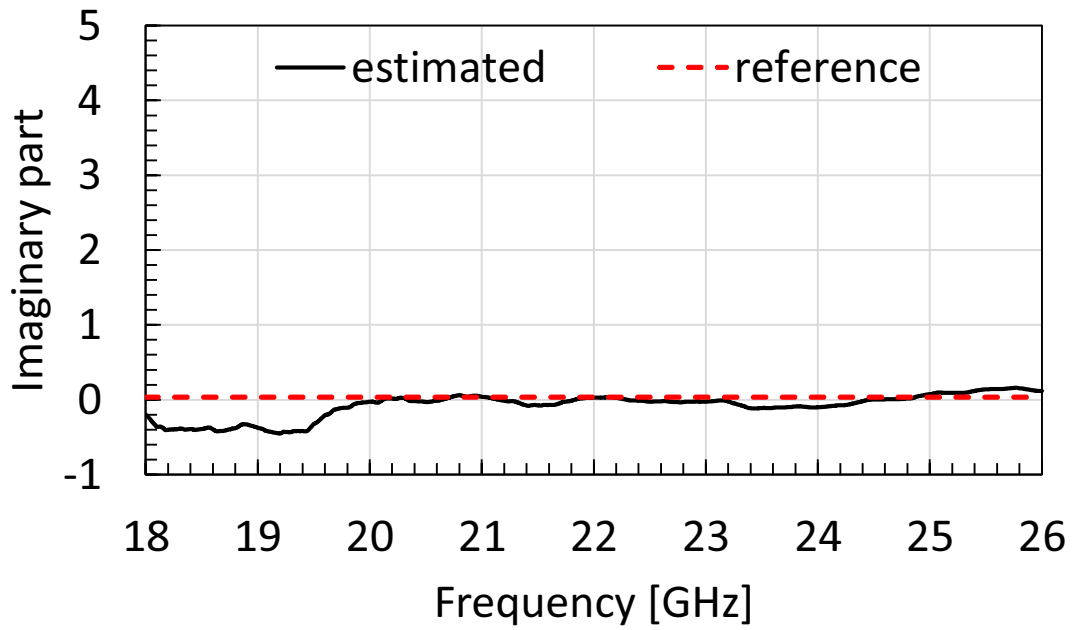


(b) Imaginary parts of water ϵ_r

Figure 5.15: Complex relative permittivity of water estimated from the fully filled container- Case II.



(a) Real parts of acrylic ϵ_r



(b) Imaginary parts of acrylic ϵ_r

Figure 5.16: Complex relative permittivity of acrylic estimated from the partially filled container.

5.5 Conclusions

In this chapter, a process to estimate water and water-based liquid's relative complex permittivity from a container's complex far field scattering quantity and the required scattering analysis have been proposed. When the space for the liquid of the container is thick enough, a simple multiple reflection coefficient model for the container can be formed to enable a direct calculation of the wanted relative permittivity. The method has been verified by estimating water's relative permittivity and promising results have been obtained. However further improvements are needed to get a more accurate value of the relative permittivity.

Chapter 6

Concluding remarks

In this work, a new free space method for dielectric permittivity estimation of solid and water-based dielectric materials has been proposed and verified.

At first, a high frequency method based on Kirchhoff approximation for electromagnetic scattering far field estimation was proposed. As shown in Chapter 3, the case of a cuboid illuminated by a TE polarized electromagnetic plane wave was considered. Equivalent currents were established using the reflected wave. In the case of dielectric cuboids, a ray tracing technique was used to include the effect of the multiple internal bouncing waves. Several PEC and dielectric cuboids were used to verify the proposed scattering analysis. Good agreements have been observed. The proposed method has proved to be quite accurate around the specular reflection direction. By using the reflected wave to estimate the equivalent currents, the method is able to calculate scattering far field from dielectric objects, while classical methods such as PO and GTD cannot be applied. Thus it opens the way to analyze the scattering far field from dielectric objects to obtain more desirable information such as the object's dielectric permittivity. This method may be used to study the scattering phenomenon from dielectric polyhedrons or more general edged objects.

The scattering analysis in Chapter 3 was applied directly to Chapter 4 and revealed the relation between the complex scattering quantity and the dielectric permittivity of solid samples and other known information. The relation is further

analyzed to devise an iterative process in order to extract the relative permittivity from the measured scattering data. An algorithm was developed to calculate for the relative permittivity without knowing much about the material's dielectric property in advance solving the multiple value difficulty. The proposed method was applied on several material samples. Dielectric permittivities were successfully estimated and compared to the results by the commercially available open-ended coaxial probe method and other references. Good agreements were observed. Under limited sense, the proposed method proved to be more accurate than the referred open-ended coaxial probe method. With the proved accuracy, stability and feasibility in dealing with non-magnetic solid materials, the method is being used to provide material information for other studies involving radar target reconstruction, propagation estimation and scattering analysis in the same laboratory. Further upgrades of the method may include stability and accuracy improvements.

Chapter 5 is an expansion into the realm of water and water-based liquids. Since liquids need containers, the effect from a container was included in the scattering analysis. A decomposition was proposed to separate unwanted scattering contributions from the measured scattering quantities. Based on the theory developed in Chapter 3, the validity of the proposed decomposition was confirmed. Based on the structure of the container and the lossy nature of water in liquids, two reflection coefficient models were proposed to calculate the scattering quantities and to establish a direct analytic relation between the dielectric permittivity of water and known information. Later, a procedure for dielectric permittivity estimation on water and water-based liquids are described. The procedure is verified by estimating water permittivity from an acrylic container and inversely. The results contain measurement errors so they oscillates strongly, however the average values agree well with references.

In conclusion, a broadband dielectric permittivity estimation technique has been developed successfully in the form of a free space method with many advantages based on the scattering analysis using Kirchhoff approximation. The method is

promising in areas where dielectric permittivity characterization of solid material is required. With improvements, the method also can be used in practice to deal with liquids. The scattering analysis developed as the foundation for the estimation process is also a new way to calculate the scattering far field from dielectric objects that can be applied in other areas.

Acknowledgment

I would like to take this opportunity to express my gratitude to Prof. Hiroshi Shirai for his supervision of this work. I have duly noticed and appreciated his kindnesses and patience over these years. He has set a standard of professional and ethical excellence to emulate. His continued guidance and support led me to the right way.

I also want to thank Prof. Keiji Goto from the National Defense Academy, Prof. Kazuya Kobayashi and Prof. Kiyotaka Yamamura from Chuo University for their advices and comments that led to important improvements in this thesis and my research.

I would like to express my deepest gratitude to my family and friends, especially dad, mom, my Secret, Mrs. Le Cam Nhung, Mr. Fujita Keisuke, Mrs. Yoshihara, Mr. Quang Ngoc Hieu, Mrs. Phan Quynh Hoa and Mr. Tei Si Sai. The encouragement from them is the main source of motivation and resilience for me to overcome tough times, to finish the research and to write this thesis.

References

- [1] A. R. Von Hippel, *Dielectric Materials and Applications*, Artech House Publication, 1995.
- [2] K. Watanabe, Y. Taka and O. Fujiwara, “Estimation of alcohol concentration of red wine based on Cole-Cole plot,” *IEEJ Transactions on Fundamentals and Materials*, vol. 129, iss. 5, pp. 352–356, 2009.
- [3] J. Sabburg, J. A. R. Ball and N. H. Hancock, “Dielectric behavior of moist swelling clay soils at microwave frequencies,” *IEEE Transactions on Geoscience and Remote Sensing*, vol. 35, no. 3, pp. 784-787, May 1997.
- [4] J. R. Wang and T. J. Schmugge, “An empirical model for the complex dielectric permittivity of soils as a function of water content,” *IEEE Transactions on Geoscience and Remote Sensing*, vol. GE-18, no. 4, pp. 288-295, Oct. 1980.
- [5] N. Tagami et al., “Dielectric properties of epoxy/clay nanocomposites - effects of curing agent and clay dispersion method,” *IEEE Transactions on Dielectrics and Electrical Insulation*, vol. 15, no. 1, pp. 24–32, Feb. 2008.
- [6] E. M. Purcell, *Electricity and Magnetism*, McGraw-Hill Co., 1965.
- [7] C. A. Balanis, *Advanced Engineering Electromagnetics*, 2nd ed, John Wiley & Sons Inc., 2011.
- [8] R. M. Redheffer, “The measurement of dielectric constant,” in *Techniques of microwave measurements*, C. G. Montgomery, Ed., ch.10, pp. 561–676, McGraw-

Hill, New York, 1947.

- [9] H. E. Bussey, “Measurement of RF properties of materials – A survey,” *Proc. of the IEEE*, vol. 55, no. 6, pp.1046–1053, June 1967.
- [10] A. C. Lynch, “Precise measurements on dielectric and magnetic materials,” *IEEE Trans. Instrumentations and Measurement*, vol. IM-23, no. 4, pp. 425–431, Dec. 1974.
- [11] L. F. Chen et. al, *Microwave Electronics: Measurements and Materials Characterization*, John Wiley & Sons, 2004.
- [12] J. Baker-Jarvis et. al, “Measuring the permittivity and permeability of lossy materials: Solids, liquids, metals, building materials, and negative-index materials,” *NIST Tech. Note 1536*, NIST Publication, 2005.
- [13] J. Krupka, “Frequency domain complex permittivity measurements at microwave frequencies,” *Meas. Sci. Technol.*, vol. 17, pp. 55–70, 2006.
- [14] C. K. Campell, “Free space permittivity measurements on dielectric materials at millimeter wavelengths,” *IEEE Trans. Instrumentations and Measurement*, vol. 27, no. 1, pp. 54–58, March 1978.
- [15] D. K. Ghodgaonkar, V. V. Varadan and V. K. Varadan, “A free space method for measurement of dielectric constants and loss tangents at microwave frequencies,” *IEEE Trans. Instrumentations and Measurement*, vol. 37, no. 3, pp. 789–793, June 1989.
- [16] D. K. Ghodgaonkar, V. V. Varadan and V. K. Varadan, “Free space measurement of complex permittivity and complex permeability of magnetic materials at microwave frequencies,” *IEEE Trans. Instrumentations and Measurement*, vol. 39, no. 2, pp. 387–394, April 1990.
- [17] R. Grignon, M. N. Afsar, Y. Wang and S. Butt, “Microwave broadband free-space complex dielectric permittivity measurements on low loss solids,” *Proc.*

- of 2003 Instrumentation and Measurement Technology Conference, vol. 1, pp. 865–870, May 2003.
- [18] U. C. Hasar and C. R. Westgate, “A broadband and stable method for unique complex permittivity determination of low-loss materials,” *IEEE Trans. Microwave Theory and Techniques*, vol. 57, no. 2, pp. 471–477, Feb. 2009.
- [19] A. Nicolson and G. F. Ross, “Measurement of the intrinsic properties of materials by time domain techniques,” *IEEE Trans. Instrum. Meas.*, IM-19(4), pp.377–382, 1970.
- [20] J. Baker-Jarvis et. al, “Improved technique for determining complex permittivity with the transmission/reflection method,” *IEEE Trans. on Microwave Theory and Techniques*, vol. 38, no.8, pp.1096–1103, 1990.
- [21] Keysight Technologies, Models in the N1500A and 85071E Materials Measurement Software.
- [22] S. A. Schelkunoff, “Some equivalence theorems of electromagnetics and their application to radiation problems,” *Bell Sys. Tech. J.*, no.15, pp. 92–112, 1936.
- [23] J. A. Stratton and L. J. Chu, “Diffraction theory of electromagnetic waves,” *Phys. Rev.*, vol. 56, iss. 1, 1939.
- [24] B. B. Baker and E. T. Copson, *The Mathematical Theory of Huygens’ Principle*, Oxford Univ. Press 1939.
- [25] C. J. Bouwkamp, “Diffraction theory,” *Rep. Prog. Phys.*, vol. 17, iss. 1, 1954.
- [26] P. Y. Ufimtsev, *Fundamentals of the Physical Theory of Diffraction*, Wiley-IEEE Press, 2007.
- [27] T. Murasaki and M. Ando, “Equivalent edge currents by the modified edge representation: Physical optics components,” *IEICE Trans. Electron.*, vol. E75–C (5), pp. 617–626, May 1992.

- [28] M. Oodo, T. Murasaki and M. Ando, “Errors of physical optics in shadow region –Fictitious penetrating rays–,” *IEICE Trans. Electron.*, vol. E77–C (6), pp. 995–1004, June 1994.
- [29] T. Shijo, L. Rodriguez and M. Ando, “The modified surface normal vectors in the physical optics,” *IEEE Trans on Antennas and Propagation*, vol. 56, no. 12, pp. 3714–3722, Dec. 2008.
- [30] J. B. Keller, “Geometrical theory of diffraction,” *J. Opt. Soc. Am.*, vol. 52, pp. 116–130, February, 1962.
- [31] J. A. Stratton, *Electromagnetic Theory*, McGraw-Hill Co., 1941.
- [32] R. A. Ross, “Radar cross section of rectangular flat plates as a function of aspect angle,” *IEEE Trans on Antennas and Propagation*, vol. AP-14, no. 3, pp. 329–335, May, 1966.
- [33] A. N. Nguyen and H. Shirai, “Electromagnetic scattering analysis from rectangular dielectric cuboids –TE polarization–,” *IEICE Trans. Electron.*, vol. E99–C, no. 1, pp. 11–17, 2016.
- [34] H. Shirai, Y. Hiramatsu and M. Suzuki, “Reconstruction of polygonal cylindrical targets with curved surfaces from their monostatic RCS,” *IEICE Trans. Electron.*, vol. E88–C, no. 12, pp. 2289–2294, 2005.
- [35] G. P. Pells, R. Heidinger, A. Ibarra-Sanchez, H. Ohno and R. H. Goulding, “An intercomparison of techniques for measuring dielectric permittivity and loss over a wide frequency range,” *Journal of Nuclear Materials*, vol. 191, pp. 535–538, 1992.
- [36] Agilent Technology, 85070 Dielectric Measurement Kit Manual, July, 2013.
- [37] A. Stogryn, “Equations for Calculating the Dielectric Constant of Saline Water,” *IEEE Trans. on Microwave Theory and Techniques*, vol. 19, iss. 8, pp. 733–736, Aug. 1971.

List of Publications

Journal Papers

- [1] A. N. Nguyen and H. Shirai, “Electromagnetic Scattering Analysis from Rectangular Dielectric Cuboids – TE polarization –,” *IEICE Trans. Electron.*, vol. E99-C, no. 1, pp.11–17, Jan. 2016.
- [2] A. N. Nguyen and H. Shirai, “A Free Space Permittivity Measurement at Microwave Frequencies for Solid Materials,” to be published in *IEICE Trans. Electron.*, vol. E100-C, no. 1, pp. 52–59, Jan. 2017.

International Conference Papers

- [1] A. N. Nguyen and H. Shirai, “Electromagnetic Wave Scattering from Lossy Polygonal Cylinders,” *Proc. of 2013 International Symposium on Electromagnetic Theory (URSI-EMTS 2013)*, pp. 816–819, Hiroshima, Japan, May 2013.
- [2] A. N. Nguyen and H. Shirai, “High Frequency Scattering Analysis of Dielectric Surfaces – TM Incidence Case,” *Proc. of 2013 Asia-Pacific Microwave Conference (APMC 2013)*, pp. 294–296, Seoul, Korea, Nov. 2013.
- [3] A. N. Nguyen and H. Shirai, “Electromagnetic Wave Scattering from Dielectric Bodies with Equivalent Current Method,” *Proc. of 2013 In-*

ternational Conference on Electromagnetics in Advanced Applications (ICEAA 2013), pp. 744–747, Turin, Italy, Sept. 2013.

- [4] A. N. Nguyen and H. Shirai, “A Numerical Method for the Estimation of Relative Permittivity of Dielectric Materials,” *Proc. of 2015 International Conference on Electromagnetics in Advanced Applications* (ICEAA 2015), pp. 125–128, Turin, Italy, Sept. 2015.

Domestic Conference Papers

- [1] A. N. Nguyen and H. Shirai, “High Frequency Scattering Field Calculation from Dielectric Surfaces,” *Proc. of 2013 IEICE General Conference*, pp. 85–90, March 2013.
- [2] A. N. Nguyen and H. Shirai, “Inverse Numerical Calculation to Determine Relative Permittivity of Lossy Dielectric Materials,” *Technical Report on Electromagnetic Theory*, IEE Japan, EMT-14-139, Nov. 2014.
- [3] A. N. Nguyen and H. Shirai, “Dielectric Permittivity Estimation Based on Free Space Method,” to be presented at *2017 IEICE General Conference*, Nagoya, Japan.